



Hall and photoluminescence studies of effects of the thickness of an additional $\text{In}_{0.3}\text{Ga}_{0.7}\text{As}$ layer in the center of $\text{In}_{0.15}\text{Ga}_{0.85}\text{As}/\text{Al}_{0.25}\text{Ga}_{0.75}\text{As}/\text{GaAs}$ high electron mobility transistors

Feng Zhao^a, Chongyang Liu^a, Shu Yuan^{a,*}, Jian Jiang^b, Michael Chan^c

^a School of Materials Engineering, Nanyang Technological University, Singapore 639798, Singapore

^b MBE Technology Pte. Ltd., 14 Science Park Drive, Science Park II, Singapore 118226, Singapore

^c Department of Electronic & Information Engineering, The Hong Kong Polytechnic University, Hung Hom, Kowloon, Hong Kong

Abstract

In order to reduce the noise and carrier–donor scattering and thereby increase the carrier mobility of the pseudomorphic AlGaAs/InGaAs high electron mobility transistors (pHEMTs), we have grown $\text{Al}_{0.25}\text{Ga}_{0.75}\text{As}/\text{In}_{0.15}\text{Ga}_{0.85}\text{As}/\text{In}_{0.3}\text{Ga}_{0.7}\text{As}/\text{GaAs}$ pHEMTs with varied $\text{In}_{0.3}\text{Ga}_{0.7}\text{As}$ thickness, and studied the effects of the $\text{In}_{0.3}\text{Ga}_{0.7}\text{As}$ thickness on the electron mobility and sheet density by Hall measurements and photoluminescence measurements. We calculated the electron and hole subbands and obtained good agreement between calculated and measured PL energies. It was found that the additional $\text{In}_{0.3}\text{Ga}_{0.7}\text{As}$ layer could be used to reduce the carrier–donor scattering, but due to the increased interface roughness as the $\text{In}_{0.3}\text{Ga}_{0.7}\text{As}$ layer becomes thicker, the interface scattering reduced the electron mobility. An optimal thickness of the $\text{In}_{0.3}\text{Ga}_{0.7}\text{As}$ was found to be 2 nm. © 2002 Published by Elsevier Science Ltd.

Keywords: AlGaAs/InGaAs/GaAs pHEMTs; Hall measurement; PL measurement; Electron mobility

1. Introduction

Pseudomorphic AlGaAs/InGaAs high electron mobility transistors (pHEMTs) grown on GaAs substrates have been widely used in wireless communications [1,2]. Usually a single InGaAs quantum well (QW) is used as the conduction channel. One of the most important parameters is the electron mobility in the channel that affects the speed of the device. Modulation doping in the barriers separates the carriers from donors, reducing the scattering between the carriers and the ionized donors and thus increasing the carrier mobility. To further separate carriers in the QW from the donors, undoped space layers are often added between the QW and the neighbor barriers. For AlGaAs/InGaAs pHEMTs on GaAs substrates, increase of the InGaAs well thickness

reduces the spread of electron wave function outside the QW, thereby reducing the carrier–donor scattering. The noise of HEMTs also affects the device performance, and can be reduced if the carrier confinement in the QW is increased, such as increasing the indium content of the InGaAs. However, both approaches are limited by the critical thickness of the InGaAs layer. To overcome such problem, in this work we added an $\text{In}_{0.3}\text{Ga}_{0.7}\text{As}$ thin layer to an $\text{Al}_{0.25}\text{Ga}_{0.75}\text{As}/\text{In}_{0.15}\text{Ga}_{0.85}\text{As}$ strained-layer QW, and carried out Hall and PL measurements to study the effects of the thickness of this additional $\text{In}_{0.3}\text{Ga}_{0.7}\text{As}$ thin layer on the sheet carrier concentration and carrier mobility in the pHEMTs.

2. Experimental procedures

The $\text{In}_{0.15}\text{Ga}_{0.85}\text{As}/\text{Al}_{0.25}\text{Ga}_{0.75}\text{As}/\text{GaAs}$ pHEMT samples were grown by molecular beam epitaxy

*Corresponding author.

E-mail address: assyuan@ntu.edu.sg (S. Yuan).

(MBE) and their structures are shown in Table 1. An additional $\text{In}_{0.3}\text{Ga}_{0.7}\text{As}$ layer was added to the structures. For the four samples the thickness of the central $\text{In}_{0.3}\text{Ga}_{0.7}\text{As}$ layers varies from 1 to 4 nm, while the total thickness of the $\text{In}_{0.15}\text{Ga}_{0.85}\text{As}$ and $\text{In}_{0.3}\text{Ga}_{0.7}\text{As}$ QW layers is fixed at 12 nm. The rest of the structures are identical for all the four samples. The indium and aluminum contents were determined by X-ray diffraction measurements after the growth process. After growth, low temperature (12 K) PL measurements were carried out by using the 488-nm line of a 40-mW Argon laser, a closed cycle cryostat, a 0.5-m spectrometer, a thermal electric cooled silicon detector, and a lock-in amplifier. Room temperature carrier mobility and sheet carrier density were determined by Hall measurements. For all the measurements, care was taken to ensure that all samples were measured under similar conditions.

3. Results and discussion

Fig. 1 demonstrates the band structure of the $\text{Al}_{0.25}\text{Ga}_{0.75}\text{As}/\text{In}_{0.15}\text{Ga}_{0.85}\text{As}$ pHEMT with $\text{In}_{0.3}\text{Ga}_{0.7}\text{As}$ thin layer in the center. HH, E1, E2, and Ef denote the first heavy hole subband, the first and second electron subbands, and the Fermi level in the QW structure, respectively.

Shown in Fig. 2 is a typical PL spectrum taken at 12 K. Three peaks were observed from all samples. The left peak is always centered at 697 nm, corresponding to the transition at the band gap of the $\text{Al}_{0.25}\text{Ga}_{0.75}\text{As}$ barrier. The other two peaks are interband transitions from the first and second electron subbands in the

Table 1
Schematic structure of the samples used in the study

Layer	x	T (nm)	N (cm^{-3})
GaAs		200	
GaAs $\times 10$		1.5	
$\text{Al}_x\text{Ga}_{1-x}\text{As} \times 10$	0.25	18.5	
$\text{Al}_x\text{Ga}_{1-x}\text{As}$	0.25	50	
Si			$1.00\text{E} + 12$
$\text{Al}_x\text{Ga}_{1-x}\text{As}$	0.25	4	
$\text{In}_x\text{Ga}_{1-x}\text{As}$	0.15	$6 - T/2$	
$\text{In}_x\text{Ga}_{1-x}\text{As}$	0.3	T	
$\text{In}_x\text{Ga}_{1-x}\text{As}$	0.15	$6 - T/2$	
$\text{Al}_x\text{Ga}_{1-x}\text{As}$	0.25	4	
Si			$4.00\text{E} + 12$
$\text{Al}_x\text{Ga}_{1-x}\text{As}$	0.25	35	
GaAs		5	$5.00\text{E} + 18$

An $\text{In}_{0.3}\text{Ga}_{0.7}\text{As}$ layer with different thickness was sandwiched in the center of the $\text{In}_{0.15}\text{Ga}_{0.85}\text{As}/\text{Al}_{0.25}\text{Ga}_{0.75}\text{As}/\text{GaAs}$ pHEMT. The thickness of the $\text{In}_{0.3}\text{Ga}_{0.7}\text{As}$ layer varies from 1 to 4 nm.

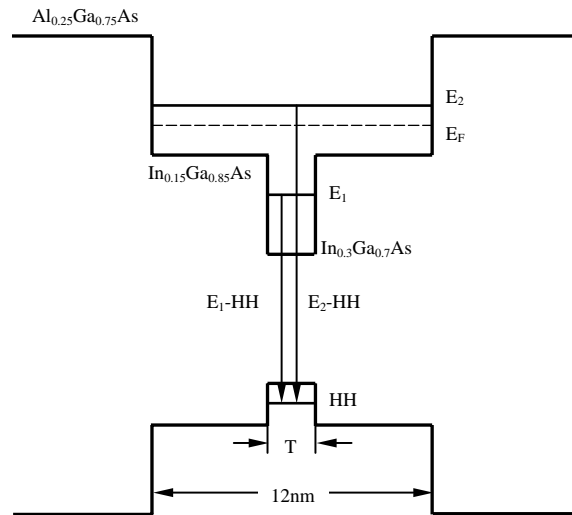


Fig. 1. Schematic band diagram of the HEMT samples. HH, E1, E2, and Ef denote the first heavy hole subband, the first and second electron subbands, and the Fermi level in the QW structure, respectively.

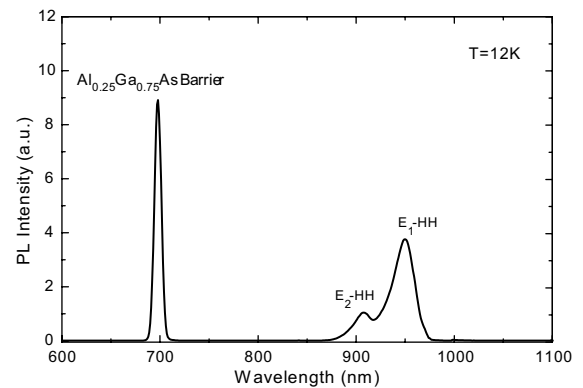


Fig. 2. PL spectrum taken at 12 K. The left peak is from the $\text{Al}_{0.25}\text{Ga}_{0.75}\text{As}$ barriers, while the right two peaks are assigned to the transitions from the first and second conduction bands to the first heavy hole.

conduction band to the ground heavy hole subband. This assignment was confirmed by a calculation of the interband transition energies. The interband transition from the second electron subband to the first heavy hole (photo-generated hole) has been reported previously in $\text{InGaAs}/\text{InAlAs}/\text{InP}$ HEMTs as well as $\text{AlGaAs}/\text{InGaAsGaAs}$ pHEMTs [3–5].

A comparison of experimental and calculated PL energies of the interband transitions is shown in Fig. 3. Good agreement is obtained for the E1–HH transition,

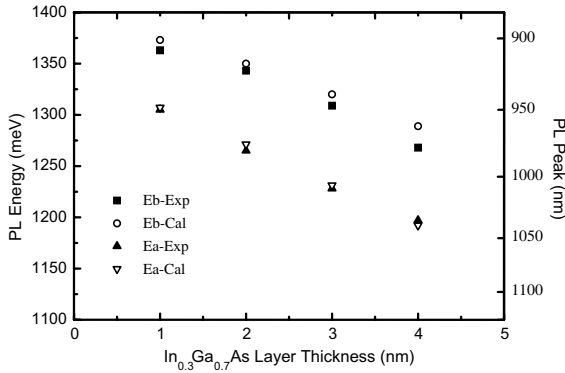


Fig. 3. PL peak energy as a function of the $\text{In}_{0.3}\text{Ga}_{0.7}\text{As}$ layer thickness. Both experimental and calculated PL energies are plotted for comparison.

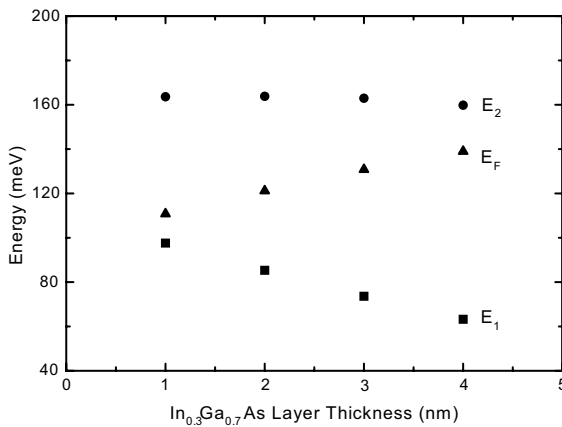


Fig. 4. Calculated electron conduction bands and Fermi level as a function of the $\text{In}_{0.3}\text{Ga}_{0.7}\text{As}$ layer thickness. While the ground state decreases significantly with increasing $\text{In}_{0.3}\text{Ga}_{0.7}\text{As}$ layer thickness, the second level is relatively insensitive. The Fermi level keeps increasing.

while reasonable agreement is achieved for the E2–HH transitions. With increase of the $\text{In}_{0.3}\text{Ga}_{0.7}\text{As}$ thickness, the electron and hole subband levels decrease, therefore, the transition energy decreases.

For the two electron subbands, the ground state is more sensitive than the second one to the thickness of the embedded layer, as shown in Fig. 4. The calculated electron wave function associated with the second level (E2) does not show noticeable change with the addition of the embedded layer. Electron wave function associated with the first electron subband in the $\text{In}_{0.15}\text{Ga}_{0.85}\text{As}/\text{Al}_{0.25}\text{Ga}_{0.75}\text{As}$ QW with ($T = 2$ nm) and without ($T = 0$ nm) the $\text{In}_{0.3}\text{Ga}_{0.7}\text{As}$ layer in the center is shown in Fig. 5. For the absence of the additional $\text{In}_{0.3}\text{Ga}_{0.7}\text{As}$ layer, the confinement profile is sym-

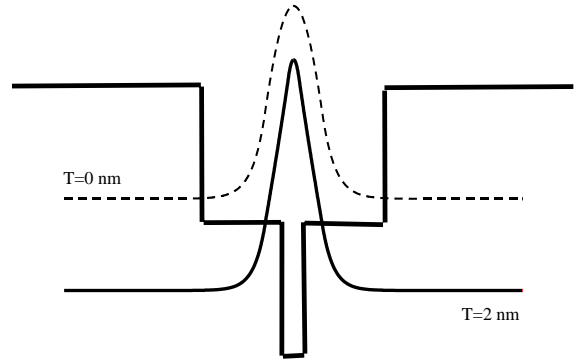


Fig. 5. Electron wave function associated with the first electron subband in the $\text{In}_{0.15}\text{Ga}_{0.85}\text{As}/\text{Al}_{0.25}\text{Ga}_{0.75}\text{As}$ QW with (—) and without (---) the $\text{In}_{0.3}\text{Ga}_{0.7}\text{As}$ layer in the center. For the absence of the additional $\text{In}_{0.3}\text{Ga}_{0.7}\text{As}$ layer, the confinement profile is symmetric inside the well, and no 2-D electron gas concentration is formed across the interface between the InGaAs and AlGaAs . The electrons do not concentrate near the center and the electron wave function will spread around the well. While with the additional $\text{In}_{0.3}\text{Ga}_{0.7}\text{As}$ QW, the ground state electrons are slightly more trapped to the center, thereby having less scattering with ionized donors in the $\text{Al}_{0.25}\text{Ga}_{0.75}\text{As}$ barriers.

metric inside the well, and no 2-D electron gas concentration is formed across the interface between the $\text{InGaAs}/\text{AlGaAs}$. The electrons do not concentrate near the center and the electron wave function will spread around the well. While with the additional $\text{In}_{0.3}\text{Ga}_{0.7}\text{As}$ QW, the ground state electrons are slightly more trapped to the center so as to be more away from the ionized donors in the $\text{Al}_{0.3}\text{Ga}_{0.7}\text{As}$ layer, thereby having less scattering with them.

The model for calculating the subbands and Fermi level is based on the envelope function scheme with the Ben-Daniel and Duke model [6] using a position dependent effective mass; the QW subband edge in the Γ -valley can be calculated by the 1-D Schrödinger-like equation. The envelope function $\Psi_{r\ell}(z)$ and eigen energy $E_{r\ell}$ can be solved by the following equation:

$$-\frac{\hbar^2}{2} \frac{d}{dz} \left[\frac{1}{m_r^*(z)} \frac{d\Psi_{r\ell}(z)}{dz} \right] + U_r(z)\Psi_{r\ell}(z) = E_{r\ell}\Psi_{r\ell}(z), \quad (1)$$

where $\ell = 1, 2, \dots$ are the QW subband levels for either the electrons, heavy holes, or light holes, respectively, $m_{\perp r}^*(z)$ is the carrier effective mass in the z direction, $E_{r\ell}$ is the subband-edge energy. Eq. (1) is solved numerically using a finite difference method. It should be noted that the confinement profiles for electrons, heavy holes and light holes will be further modified according to the carrier distribution into the QW. The Schrödinger equation and the Poisson equation are solved numerically for a self-consistent solution.

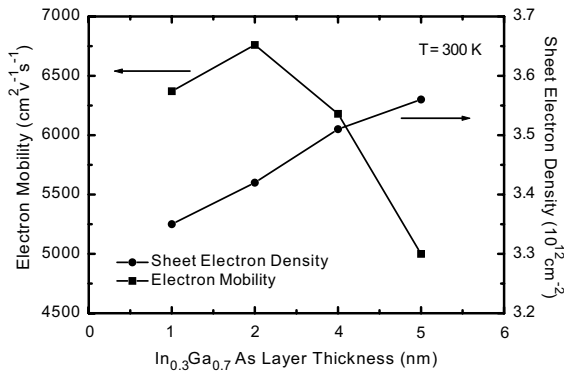


Fig. 6. Electron mobility and sheet density as a function of the $\text{In}_{0.3}\text{Ga}_{0.7}\text{As}$ layer thickness determined by Hall measurements.

An improved electron mobility is expected from the additional $\text{In}_{0.3}\text{Ga}_{0.7}\text{As}$ QW. However, when this layer becomes thicker and thicker, the interfaces between it and the $\text{In}_{0.15}\text{Ga}_{0.85}\text{As}$ layer become rougher and rougher due to growth-related problems, and the interface roughness causes some scattering, therefore reducing the electron mobility. In our work an optimal $\text{In}_{0.3}\text{Ga}_{0.7}\text{As}$ layer thickness for maximum carrier mobility is found to be around 2 nm, as shown in Fig. 6. The Fermi level, however, increases with the increase of the $\text{In}_{0.3}\text{Ga}_{0.7}\text{As}$ layer thickness, as the sheet electron concentration increases with the $\text{In}_{0.3}\text{Ga}_{0.7}\text{As}$ layer thickness. Since the second subband is relatively insensitive to the $\text{In}_{0.3}\text{Ga}_{0.7}\text{As}$ layer thickness, the increased Fermi level with the thickness indicates that most electrons occupy the E1 level.

4. Conclusion

In this work, the effects of the varied $\text{In}_{0.3}\text{Ga}_{0.7}\text{As}$ thickness on the electron mobility and sheet density in the $\text{Al}_{0.25}\text{Ga}_{0.75}\text{As}/\text{In}_{0.15}\text{Ga}_{0.85}\text{As}/\text{In}_{0.3}\text{Ga}_{0.7}\text{As}/\text{GaAs}$ p-HEMTs were studied by Hall and PL measurements. By calculating the electron and hole subbands, good agreement is obtained between calculated and measured PL energies. It was found that the additional $\text{In}_{0.3}\text{Ga}_{0.7}\text{As}$ layer could reduce the carrier-donor scattering. But due to increased interface roughness as the $\text{In}_{0.3}\text{Ga}_{0.7}\text{As}$ layer becomes thicker, the interface scattering reduces the electron mobility. The optimal thickness of the $\text{In}_{0.3}\text{Ga}_{0.7}\text{As}$ layer was found to be 2 nm.

Acknowledgements

The authors thank Prof. H.S. Fong and Dr. B.S. Ooi for their continuous support of this work.

References

- [1] Grundbacher R, Ketterson AA, Kao YC, Adesida I. IEEE Trans Electron Devices 1997;44:2136.
- [2] Somerville MH, Del Alamo JA, Saunier P. IEEE Trans Electron Devices 1998;45:1883.
- [3] Li H, Wu J, Liang ZWJ, Xu B, Jiang C, Gong Q, Liu F, Zhou W. J Cryst Growth 1998;186:309.
- [4] Colvard C, Mouri N, Lee H, Ackley D. Phys Rev B 1989;39:8033.
- [5] Gilperez JM, Sanchez-Rojas JL, Munoz E, Colleja E, David JPR. Appl Phys Lett 1995;66:748.
- [6] BenDaniel DJ, Duke CB. Phys Rev 1966;152:683.